Numerical investigation of heat transfer by natural convection and radiation in a cavity with participating media

C.U. Mendoza, cristian.uriel@fem.unicamp.br[1]
C.T Salinas, csalina@fem.unicamp.br[1]
J.M. Armengol, jan.mateu.armengol@gmail.com[1]
R. Beicker, rbeicker@gmail.com[1]
R.G. Santos, roger7@fem.unicamp.br[1]

[1]UNICAMP

Abstract: *This paper deals with the numerical solution of combined heat transfer by radiation and natural convection in a square cavity under normal room conditions, filled with an absorbing-emitting and isotropic scattering medium. The finite volume method (FVM) has been adopted to solve the governing equations of natural convection. In turn, the discrete ordinates method (DOM) is applied to solve the radiative transfer equation (RTE), using a Tn6 angular quadrature. Natural convection and radiative transfer equations are solved simultaneously. The numerical model is validated by comparison with results taken from literature. In this work, Nusselt number and temperature and velocity fields are numerically studied for scattering albedos between* $0.0 - 1.0$ *ranging the Rayleigh number and the optical thickness. The results show that the effects of radiation are greater when the Rayleigh number increases. Similarly, it is shown that the influence of scattering albedo is stronger for cavities with higher Rayleigh numbers and optical thicknesses.*
Keywords: *Numerical Simulation, Natural Convection, Radiative Heat Transfer, Finite Volumes, Discrete Ordinates Method.*

1. NOMENCLATURE

c_p	Specific heat capacity, $J \cdot kg^{-1} \cdot K^{-1}$	t	Time, s
g	gravity, g = 9.81 ms^{-2}	T	Temperature, K
H	Cavity height and width, m	u	Horizontal velocity, $m \cdot s^{-1}$
I	Radiative intensity $W\ m^{-2}\ sr^{-1}$	v	Vertical velocity, $m \cdot s^{-1}$
m	Angular direction	V	Volume, m^3
M	Number of total angular directions	W	Quadrature weight of vector director
n	Director vector of area	x	Horizontal coordinate, m
Nu	Nusselt number	y	Vertical coordinate, m
$\bar{P}$	Thermodynamic average pressure, Pa	**Greek symbols**	
Pl	Plank number	α	Thermal diffusivity
Pr	Prandt number	$\bar{\beta}$	Thermal expansion coefficient, K^{-1}
q	Heat flux, $W\ m^{-2}$	β	Extinction coefficient, m^{-1}
r	Position vector , m	$\bar{\epsilon}$	Non-dimenional temperature difference
R	Gas constant for air, 287 $J \cdot (kg \cdot K)^{-1}$		parameter, $\bar{\epsilon} = (T_h - T_c)/(T_h + T_c)$
Ra	Rayleigh number	ε	Surface emissivity

κ	Absorption coefficient, m^{-1}	m	m discrete direction
λ	Thermal conductivity, $W \cdot m^{-1} \cdot K^{-1}$	$'$	Incident direction
μ	Dynamic viscosity, $Pa \cdot s$	**Subscripts**	
$\bar{\mu}$	x- projection of the director vector	b	Black body
Ω	Director vector	c	Cold wall
ρ	Density, $kg \cdot m^{-3}$	Cv	Convectivet
σ	Scattering coefficient, m^{-1}	E	East
$\bar{\sigma}$	Stephan-Boltzman constant	h	Hot wall
τ	Optical thickness	N	North
$\bar{v}$	Kinematic viscosity, $m^2 \cdot s^{-1}$	o	Initial condition
ω	Scattering albedo, $m^2 \cdot s^{-1}$	P	Node
$\bar{\omega}$	Intensity interpolation scheme constant	ref	Reference value
Superscripts		Rd	Radiative
$*$	Dimensionless variable		

2. INTRODUCTION

The phenomenon of natural convection is essential for the functioning of several engineering applications, such as double-glazed windows, solar collectors, cooling devices for electronic gears, HVAC (heating, ventilation and air-conditioning) systems, crystal growth in liquids, and fire spreading. Thus, many works about natural convection are performed. Among many academic studies, natural convection in rectangular cavities filled with air has proved to be an excellent vehicle in light of both numerical and empirical analyses (Ampofo and Karayiannis (2003); Tian and Karayiannis (2000); Salat *et al.* (2004); Betts and Bokhari (2000); Yin *et al.* (1978)).

A benchmark study of numerical solutions for natural convection in a two-dimensional closed square cavity filled with air was done by de Vahl Davis and Jones (1983). They worked on this physical problem by matching the second-order finite-differences method with the Richardson extrapolation scheme. In his work, Churchill (1983) suggested an experimental approach - formulations and graphics - to determine the Nusselt number (Nu) at distinct Rayleigh numbers and situations, according to some empirical and numerical results. Over the last few years, owing to the development of algorithms more efficient and computers with high processing rates, solutions of the 2-D and 3-D laminar equations have been solved for values of Ra in wide ranges, as we can see in the works of Upson *et al.* (1980) and Saitoh and Hirose (1989).

Many papers that combine radiation and natural convection in closed rectangular cavity with air can be found in the literature (Sharma *et al.* (2007); Velusamy *et al.* (2001); Akiyama and Chong (1997); Behnia *et al.* (1990)). For example, Akiyama and Chong (1997) studied the relationship between natural convection and radiation in a square cavity filled with air. Their results have shown that the surface radiation changes considerably the temperature distribution and the flow templates, particularly at uppermost Ra. So, the radiative heat transfer represent a high percentage of the overall heat flux. Furthermore, this part of heat flux improves with the increment of fluid emissivity.

However, works which analyze the phenomena of natural convection and radiation in cavity filled with air considering participating media are less common, given the high quantity of computational resources required to process it (Colomer *et al.* (2004); Fusegi and Farouk (1989); Fiveland (1988)). Tan and Howell (1991) studied combined radiation and natural convection in emitting, absorbing, and isotropically scattering square cavities. By means of the product integration method, the precise formulation for radiation was established and discretized (Tan (1989b)). The non-linear successive-over-relaxation iterating scheme for associated radiation and convection-conduction heat transfer problems was also applied (Tan (1989a)). In 2011, Lari *et al.* (2011) conducted a study on this specific topic considering the Bous-

sinesq approximation, steady state, and absorbing-emitting medium with gray gases. The objective of her work was to investigate the effect of radiation on total heat transfer in a square under standard conditions combined with a low temperature difference. Recently, Moufekkir *et al.* (2012) used the numerical approach to solve the natural convection and volumetric radiation in an isotropic scattering medium within a heated square cavity problem using a different version of the thermal lattice Boltzmann method. In his paper, the finite difference method was combined with the multiple relaxation time lattice Boltzmann method to work out the mass conservation, the Navier-Stokes and the energy equations. In turn, the discrete ordinates method was applied to resolve the radiative transfer equation. Done it, he studied the influence of some important parameters over the heat transfer (for example, scattering albedo, Rayleigh number and Planck number).

The present work determines the overall averaged Nusselt number, as well as, the natural convection and the radiation averaged Nusselt numbers in the presence of a low temperature difference. The problem of the square enclosure, differentially heated side walls, insulated top and bottom sides, and filled with air - participating medium and grey gas - is solved for some scattering albedos ranging the Rayleigh number and the optical thickness. The Boussinesq approach is used even as in the previously cited works. The discrete ordinates method was also applied to deal with the radiative transfer equation. It was used the assumption of constant properties - thermal conductivity, thermal diffusivity, density, dynamic and cinematic viscosity. As far as we known, there is not any published work that shows how the radiation contribution varies for the total heat transfer when ranging the scaterring albedo, the Rayleigh number and the optical thickness in an incompressible formulation only using the finite volume method to calculate the mass conservation, the Navier-Stokes and the energy equations.

3. MATHEMATICAL AND PHYSICAL MODEL

The case of study of the present work is a square cavity filled with an absorbing, emitting, and isotropic scattering gray medium whose horizontal walls are considered adiabatic and the vertical walls have a fixed temperature. The motion of fluid initially static is induced by a temperature difference between the vertical walls, setting the right and left walls at T_c and T_h respectively, as shown in Fig. 1. All walls are considered black and diffusely reflective.

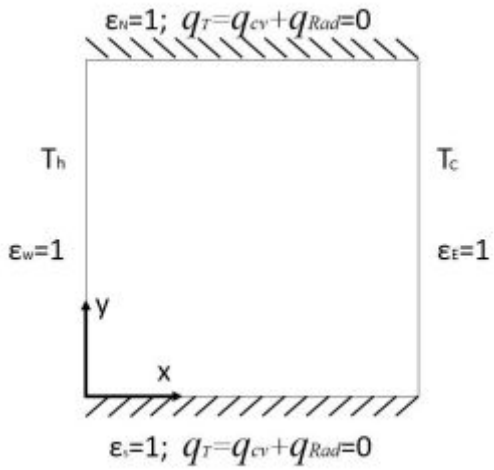

Figure 1: **Skecth of the physical model.**

The governing equations for two-dimensional flow, using the Boussinesq approximation, corresponding to mass conservation, transport of momentum in both directions and transport of energy are, respectively :

$$\frac{\partial \rho}{\partial t} + \frac{\partial (\rho u)}{\partial x} + \frac{\partial (\rho v)}{\partial y} = 0, \tag{1}$$

$$\frac{\partial (\rho u)}{\partial t} + \frac{\partial (\rho u \cdot u)}{\partial x} + \frac{\partial (\rho v \cdot u)}{\partial y} = -\frac{\partial P}{\partial x} + \frac{\partial}{\partial x}\left(\mu \frac{\partial u}{\partial x}\right) + \frac{\partial}{\partial y}\left(\mu \frac{\partial u}{\partial y}\right), \tag{2}$$

$$\frac{\partial (\rho v)}{\partial t} + \frac{\partial (\rho u \cdot v)}{\partial x} + \frac{\partial (\rho v \cdot v)}{\partial y} = -\frac{\partial P}{\partial y} + \frac{\partial}{\partial x}\left(\mu \frac{\partial v}{\partial x}\right) + \frac{\partial}{\partial y}\left(\mu \frac{\partial v}{\partial y}\right) + \rho_0 \vec{g} \bar{\beta}(T - T_0), \tag{3}$$

$$\frac{\partial (\rho T)}{\partial t} + \frac{\partial (\rho u \cdot T)}{\partial x} + \frac{\partial (\rho v \cdot T)}{\partial y} = \frac{\partial}{\partial x}\left(\frac{\lambda}{c_p} \frac{\partial T}{\partial x}\right) + \frac{\partial}{\partial y}\left(\frac{\lambda}{c_p} \frac{\partial T}{\partial y}\right) - \frac{1}{c_p} \nabla q_{Rd}. \tag{4}$$

The term $\frac{1}{c_p}\nabla q_{Rd}$ in Eq. (4) denotes the divergence of the radiative flux which can be calculated with the radiative intensity field by the expression:

$$\nabla q_{Rd} = \kappa \left(4\pi I_b(r) - \int_{4\pi} I(r,\Omega) d\Omega \right). \tag{5}$$

To obtain the intensity field to compute the Eq. (5) is necessary to solve the radiative transfer equation (RTE), which for an absorbing, emitting and isotropic scattering gray medium is determined by:

$$(\Omega\nabla) I(r,\Omega) = -\beta I(r,\Omega) + \kappa I_b(r) - \frac{\sigma}{4\pi} \int_{4\pi} I(r,\Omega') d\Omega'. \tag{6}$$

In order to generalize, the dimensionless parameters used are:

$$T^* = \frac{T - T_c}{T_h - T_c}, \quad x^* = \frac{x}{H}, \quad y^* = \frac{y}{H}, \quad u^* = \frac{uH}{\alpha_o}, \quad \text{and} \quad v^* = \frac{vH}{\alpha_o}. \tag{7}$$

The dimensionless temperature difference parameter, Plank, Prandt and Rayleigh numbers are defined as:

$$\bar{\epsilon} = \frac{T_h - T_c}{T_h + T_c}, \quad Pl = \frac{\lambda_{ref}}{4\sigma_B T_{ref}^3 H}, \quad Pr = \frac{c_p \mu_{ref}}{\lambda_{ref}}, \quad \text{and} \quad Ra = \frac{g\bar{\beta}(T_h - T_c)H^3}{\upsilon_{ref}^{-} \alpha_{ref}}. \tag{8}$$

where T_{ref} is a reference temperature defined as $T_{ref} = (T_h + T_c)/2$; and $\lambda_{ref}, \alpha_{ref}, \rho_{ref}, \mu_{ref}$ and υ_{ref} are the thermal conductivity, thermal diffusivity, density, dynamic and cinematic viscosity evaluated at T_{ref}, respectively, which are considered spatially constants. For that, the dynamic viscosity and thermal conductivity are calculated using the expressions as follows called Sutherland's law:

$$\mu(T) = \mu' \left(\frac{T}{T'} \right)^{3/2} \frac{T' + C}{T + C} \tag{9}$$

$$\lambda(T) = \mu(T) \frac{\gamma R}{(1-\gamma) Pr} \tag{10}$$

At the present work, the used values are $\mu' = 1.68\text{x}10^{-5} Kg/ms$, $T' = 273K$, $C = 110,5\ Kg/msK^{1/2}$, $\gamma = 1.4$, $R = 287J/KgK$ and $Pr = 0.71$.

The heat transfer through the cavity is characterized by the Nusselt number, which involves the convective and radiative heat transfer effects. The local convective and radiative Nusselt numbers at the hot wall are determined as follows:

$$Nu(y)_{Cv}\Big|_{x=0} = \frac{H}{(T_h - T_c)} \frac{\partial T}{\partial x}\Big|_{x=0} \quad \text{and} \quad Nu(y)_{Rd}\Big|_{x=0} = \frac{q_{Rd}\, H}{\lambda_{ref}(T_h - T_c)}. \tag{11}$$

The average Nusselt numbers for convective and radiative effects are expressed as:

$$\overline{Nu}_{Cv}\Big|_{x=0} = \frac{1}{H} \int_0^H Nu(y)_{Cv}\Big|_{x=0} dy. \quad \text{and} \quad \overline{Nu}_{Rd}\Big|_{x=0} = \frac{1}{H} \int_0^H Nu(y)_{Rd}\Big|_{x=0} dy. \tag{12}$$

The overall averaged Nusselt number is determinated by:

$$Nu(y)_T\Big|_{x=0} = Nu(y)_{Cv}\Big|_{x=0} + Nu(y)_{Rd}\Big|_{x=0} \quad \text{and} \quad \overline{Nu}_T\Big|_{x=0} = \overline{Nu}_{Cv}\Big|_{x=0} + \overline{Nu}_{Rd}\Big|_{x=0}. \tag{13}$$

3.1 Boundary and initial conditions

The boundary conditions for the situation described in the Fig. 1 can be modeled as:

Left boundary ($x = 0$; $0 < y < H$) Isothermal, non-slip, impermeable and diffusively reflective black wall:

$$u = v = 0, \quad T_h = T_{ref}(1 + \bar{\epsilon}) \text{ and } \varepsilon_h = 1.0. \tag{14}$$

Right boundary ($x = H$; $0 < y < H$) Isothermal, non-slip, impermeable and diffusively reflective black wall:

$$u = v = 0 \quad T_c = T_{ref}(1 - \bar{\epsilon}) \text{ and } \varepsilon_c = 1.0. \tag{15}$$

Bottom ($y = 0$) and Top ($y = H$) boundaries. Adiabatic, non-slip, impermeable and diffusively reflective black wall:

$$u = v = 0, \quad q_{Cv} + q_{Rd} = 0 \text{ and } \varepsilon_s = \varepsilon_n = 1.0. \tag{16}$$

Initial conditions ($t = 0$). Stationary flow at spatially uniform temperature T_0 and pressure P_0, wherein fluid properties are computed at T_0:

$$u_0 = v_0 = 0,\ T_0 = T_{ref},\ P_0 = 101325\ Pa,\ \rho_0 = \frac{P_0}{R\,T_0},\ \mu_0 = \mu(T_0) \text{ and } \lambda_0 = \lambda(T_0). \tag{17}$$

For opaque walls that emit and reflect diffusely, the boundary conditions for RTE (Eq. 6) are calculated by:

$$I(r_w, \Omega) = \varepsilon I_b(r_w) + \frac{(1-\varepsilon_w)}{\pi} \int_{\vec{n}\cdot\Omega'<0} I(r_w, \Omega')\,|\vec{n}\cdot\Omega'|\,d\Omega'. \tag{18}$$

4. METHODOLOGY FOR THE NUMERICAL SOLUTION

In order to solve the Naver-Stokes, mass conservation and energy equations (Eq.(1)-(4)), the finite volume method (FVM) is used for their discretization applying a false transient formulation and using a fully implicit scheme for time discretization (Patankar (1980), and Versteeg and Malalasekera (2007)). The diffusive term is approximated by using central difference scheme while the hybrid scheme is used for the convective term. Due to the equations of conservation of mass and momentum are strongly coupled, the algorithm SIMPLE is implemented with a non-uniform staggered marker-and-cell (MAC) mesh, where all scalar quantities are calculated on the main grid while the components of the velocity are associated to the staggered grid. The properties C_p, ρ, λ and μ are assumed spatially constants and are evaluated at the reference temperature.

To obtain the source term in Eq.4, corresponding to the radiative flux, the intensity field is solved by RTE, for which the angular discretization is done by the discrete ordinates method (DOM) as explains Fiveland (1984) using a Tn6 quadrature as calculated in Thurgood *et al.* (1995). The FVM is used to make the spatial discretization. Thus, the intensity of the point P in the m direction can be described as a function of the intensities at the faces of the control volume as:

$$\bar{\mu_m}(A_E I_E^m - A_W I_W^m) + \bar{\xi_m}(A_N I_N^m - A_S I_S^m) = -\beta I_p^m V_p + \kappa I_{b,p}^m V_p + \left(\frac{\sigma}{4\pi}\sum_{k=1}^{M} W_k I^k\right) V_p. \tag{19}$$

The number of variables in the Eq. (19) are reduced using the linear correlation:

$$I_p^m = \bar{\omega} I_E^m + (1-\bar{\omega}) I_W^m = \bar{\omega} I_S^m + (1-\bar{\omega}) I_N^m. \tag{20}$$

where $\bar{\omega}$ is a constant between $0.0 - 1.0$. Note that $\bar{\omega}$ = 1.0 and $\bar{\omega}$ = 0.5 denote step and diamond scheme respectively. From Eq. (20) and Eq. (19), it is obtained the numerical expression used in this work:

$$I_p^m = \frac{|\bar{\mu}|\triangle y I_w^m + |\bar{\xi}|\triangle x I_s^m + \bar{\omega}\kappa I_{b,p} V_p + \bar{\omega}\left(\frac{\sigma}{4\pi}\sum\limits_{k=1}^{M} W_k I^k\right) V_p}{|\mu|\triangle y + |\xi|\triangle x + \bar{\omega}\beta V_p}. \tag{21}$$

To determine the effect of the scattering on the flow, it is introduced the single scattering albedo defined as:

$$\omega = \frac{\sigma}{\sigma + \kappa} = \frac{\sigma}{\beta}. \tag{22}$$

Note that for a non-scattering medium, ω=0.0, while ω=1.0 in a non-absorbing medium ($\kappa = 0.0$).

Similarly, the DOM is used in the boundary conditions for the RTE (Eq.18). The expression to calculate the source term in the energy equation (Eq.5) at node P which is associated to one control volume of the domain is given by the expressions used at the model of numerical implementation:

$$I_w^m = \varepsilon_w I_{b,w} + \frac{(1-\varepsilon_w)}{\pi}\sum_{k=1}^{M'} W_{k'} I_w^{k'}\,|\Omega_k'|\,. \tag{23}$$

$$\nabla q_{Rd} = \kappa\left(4\pi I_{b,p} - \sum_{k=1}^{M} W_k I_p^k\right). \tag{24}$$

The set of algebraic equations generated by the discretization of the governing equation of the flow is solved by an alternating direction implicit (ADI) iterative method. Additionally, under-relaxation parameters have been used to minimize the number of iterations required to reach the convergence criteria.

4.1 Grid sensivity and code verifications

The accuracy of the numerical results has been verified through numerous tests based on grid size covering Rayleigh numbers between $10^3 - 10^7$. The Table 1 summarizes the results for $Ra = 10^6$ and $\tau = 1.0$. The numerical analysis revealed that higher Rayleigh numbers demand refiner meshes. A non-uniform mesh of 161 x 161 nodes is selected, for which a maximum deviation of 0.1 % is obtained for the average Nusselt number.

Table 1: **Radiative and total averaged Nusselt number for $Ra = 10^6$, $Pr = 0.717$ and $\tau = 1.0$.**

		61x61	81x81	101x101	121x121	141x141	161x161	181x181	201x201
$\tau = 1.0$	Nu_{Rd}	9.577	9.563	9.557	9.554	9.553	9.528	9.525	9.522
	Nu_T	16.947	16.920	16.910	16.906	16.904	16.864	16.861	16.857

In order to verify the results obtained from the numerical model considering the radiative heat transfer effects, the Table 2 shows a comparison with values of average Nusselt number at hot wall obtained by Lari *et al.* (2011) for two different optical thicknesses and Rayleigh numbers with values of Pr=0.717, scattering albedo $\omega = 0.0$, $T_h = 310$ K, and $T_c = 290$ K. It shows a maximum deviation of 1.625%. The Figure 2 corroborates the results of the present work showing a good compatibility with the streamlines and the isotherms.

Table 2: **Comparison of the present work with the results of Lari *et al.***

		$Ra = 10^5$	$Ra = 10^6$
$\tau = 1.0$	Lari *et al.*	8.367	17.086
	Present work	8.231 (1.625 %)	16.864 (1.300 %)
$\tau = 5.0$	Lari *et al.*	6.811	14.514
	Present work	6.732 (1.160 %)	14.439 (0.517 %)

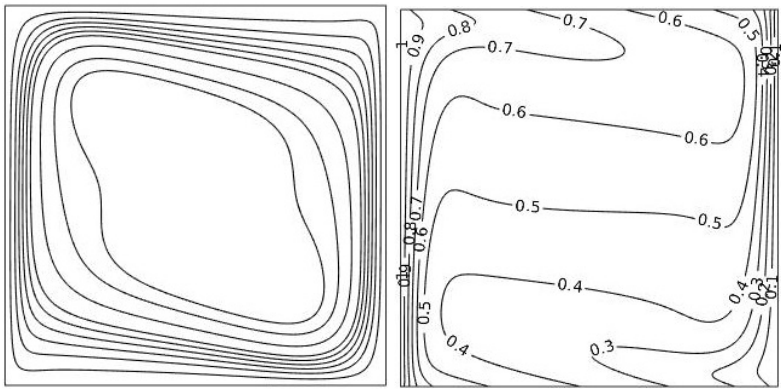

(a) (b)

Figure 2: $Ra = 10^6, Th = 310K, Tc = 290K, \tau = 1.0$ **(a) Streamlines. (b) Dimensionless Isotherms lines.**

Similarly, the Table 3 shows a comparison with results taken from Moufekkir *et al.* (2012) and Yucel *et al.* (1989) for a cavity with $Ra = 5x10^6$, $Pr = 0.71$, $Pl = 0.2$, scattering albedo $\omega = 0$ and two different optical thicknesses. The maximum deviation showed is 1.11%. It can be observed a good agreement of the results of this work with values from the literature.

Table 3: **Comparison of the present work with the results of Moufekkir *et al.* and Yucel *et al.***

		Nu_Rd	Nu_T
$\tau = 1.0$	Yucel *et al.*	31.550 (0.41 %)	39.210 (0.68 %)
	Moufekkir *et al.*	31.108 (1.00 %)	38.725 (0.57 %)
	Present work	31.421	38.945
$\tau = 5.0$	Yucel *et al.*	23.640 (1.11 %)	31.760 (0.43 %)
	Moufekkir *et al.*	23.801 (0.57 %)	31.778 (0.37 %)
	Present work	23.936	31.896

5. Results

For the purpose of keeping the flow in the laminar regime, all tests were made with a Rayleigh number between 10^4--10^7 as well as the difference of temperature between vertical walls was established at low enough value to guarantee that all considerations in the mathematical model are appropriated. To evaluate the effects of the scattering albedo on the velocity and temperature fields, tests with values between $0.0-1.0$ were made too. The Table 4 shows the average Nusselt number at the hot wall for distinct scattering albedos, two optical thicknesses and two Rayleigh numbers in a cavity filled with an absorbing, emitting, and isotropic scattering gray medium in which Pr=0.717 and the temperatures at the left and right walls are $T_h = 310$K and $T_c = 290$K respectively.

Table 4: **Radiative, convective and total average Nusselt number for different values of scattering albedo.**

		$Ra = 10^4$			$Ra = 10^7$		
		Nu_{Cv}	Nu_{Rd}	Nu_T	Nu_{Cv}	Nu_{Rd}	Nu_T
	τ=1.0	2.2055	1.7892	3.9947	13.1853	21.0650	34.2510
ω=0.0	τ=5.0	2.2248	0.8334	3.0582	13.7687	16.5181	30.2868
	τ=1.0	2.1722	1.8079	3.9800	13.3762	20.1321	33.5083
ω=0.5	τ=5.0	2.1310	0.8484	2.9794	13.2159	14.6531	27.8690
	τ=1.0	2.1617	1.8142	3.9759	13.5570	19.6613	33.2183
ω=0.7	τ=5.0	2.0956	0.8477	2.9433	13.1439	13.2263	26.3702
	τ=1.0	2.1533	1.8195	3.9728	14.1118	18.7775	32.8892
ω=1.0	τ=5.0	2.1089	0.7768	2.8857	14.2281	8.3179	22.5460
Pure convection		2.2409	0.0	2.2409	16.5924	0.0	16.5924

Table 4 shows that, for the studied cases, the influence of scattering albedo is stronger for a larger Rayleigh number and higher values of optical thickness. When scattering albedo increases, keeping constant the others parameters of the flow, the heat transfer decreases. It should be noted that these effects are more pronounced in the radiative heat transfer, while the convective effects suffer lower variations. For the case of pure convection, the variation of scattering albedo has not any effect on the flow, because this parameter is directly related to the conditions of the radiative heat transfer.

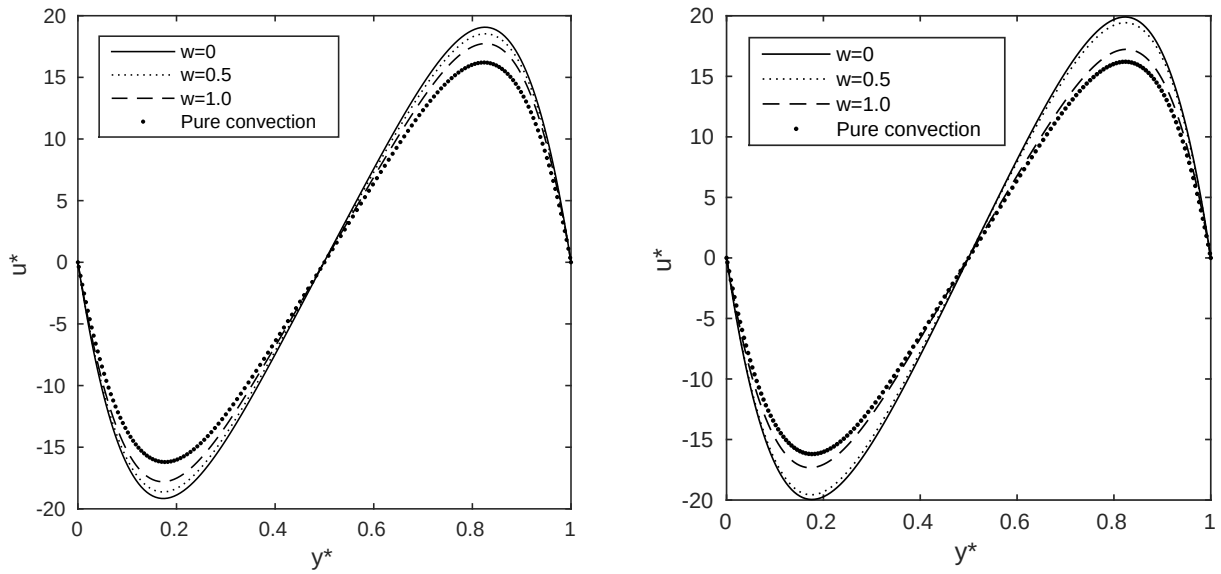

(a) (b)

Figure 3: **Dimensionless horizontal velocity profile at the mid-plane for** $Ra = 10^4$. (a) $\tau = 1.0$ (b) $\tau = 5.0$

The Figures (3) and (4) show the dimensionless horizontal velocity profile at the mid-plane of the cavity for $Ra = 10^4$ and $Ra = 10^7$ respectively. They reveal that when the scattering albedo increases, the dimensionless horizontal velocity profile at the mid-plane declines. Can be observed that , these effect is stronger for a higher Rayleigh number and a lower optical thickness.

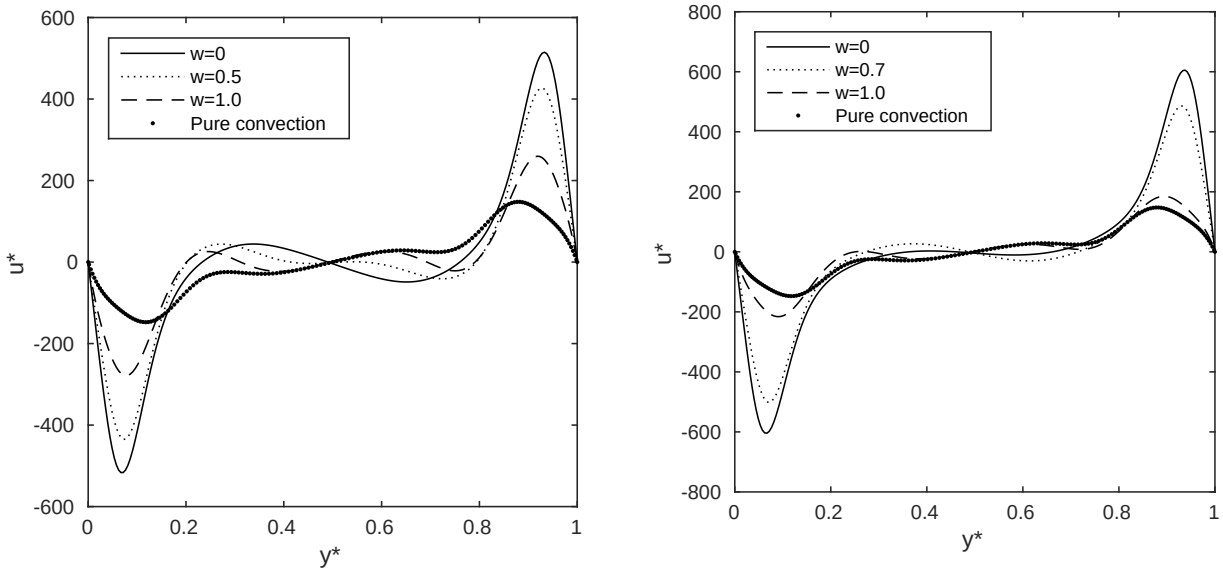

(a) (b)

Figure 4: **Dimensionless horizontal velocity profile at the mid-plane for** $Ra = 10^7$. (a) $\tau = 1.0$ (b) $\tau = 5.0$

6. CONCLUSIONS

The heat transfer by natural convection and radiation in a cavity under normal room conditions filled with an absorbing-emitting and isotropic scattering gray medium has been studied at present work. The equations of mass conservation, momentum and transport of energy have been solved by the FVM using the SIMPLE algorithm. The RTE has been discretized angularly by the DOM and spatially by the FVM to evaluate the source term in the equation of energy associated with the radiative heat transfer. The code of the present work has been verified by comparison with results of the bibliography. The heat transfer and the characteristic of the fluid were analyzed for a variation of scattering albedo in a range from 0.0 to 1.0 at different Rayleigh numbers and optical thicknesses. The next conclusions have been obtained from this study:

- For a more absorbing medium (a lower scattering albedo) flowing with the same characteristics, the heat transfer through the cavity is greater.
- The magnitudes of the velocity in a more scattering medium (a higher scattering albedo) are lower.
- The effects of scattering albedo are stronger for a flow with a higher Rayleigh number and a medium with lower optical thickness.

7. ACKNOWLEDGEMENTS

The authors wish to thanks CAPES and FAPESP for the financial support.

8. REFERENCES

Akiyama, M. and Chong, Q., 1997. "Numerical analysis of natural convection with surface radiation in a square enclosure". *Numerical Heat Transfer, Part A Applications*, Vol. 32, No. 4, pp. 419–433.

Ampofo, F. and Karayiannis, T., 2003. "Experimental benchmark data for turbulent natural convection in an air filled square cavity". *International Journal of Heat and Mass Transfer*, Vol. 46, No. 19, pp. 3551–3572.

Behnia, M., Reizes, J. and de Vahl Davis, G., 1990. "Combined radiation and natural convection in a rectangular cavity with a transparent wall and containing a non-participating fluid". *International Journal for Numerical Methods in Fluids*, Vol. 10, No. 3, pp. 305–325.

Betts, P. and Bokhari, I., 2000. "Experiments on turbulent natural convection in an enclosed tall cavity". *International Journal of Heat and Fluid Flow*, Vol. 21, No. 6, pp. 675–683.

Churchill, S., 1983. "Free convection in layers and enclosures". *Heat exchanger design handbook*, Vol. 2, No. 8.

Colomer, G., Costa, M., Consul, R. and Oliva, A., 2004. "Three-dimensional numerical simulation of convection and radiation in a differentially heated cavity using the discrete ordinates method". *International Journal of Heat and Mass Transfer*, Vol. 47, No. 2, pp. 257–269.

de Vahl Davis, G. and Jones, I., 1983. "Natural convection in a square cavity: a comparison exercise". *International Journal for numerical methods in fluids*, Vol. 3, No. 3, pp. 227–248.

Fiveland, W., 1984. "Discrete-ordinates solution of the radiative transport equation for rectangular enclosures". *Journal of Heat Transfer*, Vol. 106, pp. 699–706.

Fiveland, W., 1988. "Three-dimensional radiative heat-transfer solutions by the discrete-ordinates method". *Journal of Thermophysics and Heat Transfer*, Vol. 2, No. 4, pp. 309–316.

Fusegi, T. and Farouk, B., 1989. "Laminar and turbulent natural convection-radiation interactions in a square enclosure filled with a nongray gas". *Numerical Heat Transfer*, Vol. 15, No. 3, pp. 303–322.

Lari, K., Baneshi, S.A., Nassab, S.A.G., Komiya, A. and maruyama, S., 2011. "Combined heat transfer of radiation and natural convection in a square cavity containing participant gases". *International journal of heat and mass transfer*, Vol. 54, pp. 5087–5099.

Moufekkir, F., MOussauoui, M.A., Mezrhad, A., Naji, H. and Lemonnier, D., 2012. "Numerical prediction of heat transfer by natural convection and radiation in an enclosure filled with an isotropic scattering medium". *Journal of quantitative spectroscopy & radiative transfer*, Vol. 113, pp. 1689–1704.

Patankar, S., 1980. *Numerical heat transfer and fluid flow*. CRC Press.

Saitoh, T. and Hirose, K., 1989. "High-accuracy bench mark solutions to natural convection in a square cavity". *Computational Mechanics*, Vol. 4, No. 6, pp. 417–427.

Salat, J., Xin, S., Joubert, P., Sergent, A., Penot, F. and Le Quere, P., 2004. "Experimental and numerical investigation of turbulent natural convection in a large air-filled cavity". *International Journal of Heat and Fluid Flow*, Vol. 25, No. 5, pp. 824–832.

Sharma, A.K., Velusamy, K., Balaji, C. and Venkateshan, S., 2007. "Conjugate turbulent natural convection with surface radiation in air filled rectangular enclosures". *International journal of heat and mass transfer*, Vol. 50, No. 3, pp. 625–639.

Tan, Z., 1989a. "Combined radiative and conductive heat transfer in two-dimensional emitting, absorbing and anisotropic scattering square media". *International communications in heat and mass transfer*, Vol. 16, No. 3, pp. 391–401.

Tan, Z., 1989b. "Radiative heat transfer in multidimensional emitting, absorbing, and anisotropic scattering media—mathematical formulation and numerical method". *Journal of heat transfer*, Vol. 111, No. 1, pp. 141–147.

Tan, Z. and Howell, J.R., 1991. "Combined radiation and natural convection in a two-dimensional participating square medium". *International journal of heat and mass transfer*, Vol. 34, No. 3, pp. 785–793.

Thurgood, C.P., Pollard, A. and Becker, H.A., 1995. "The tn quadrature set for the discrete ordinates method." *Journal of Heat Transfer*, Vol. 117, pp. 1068–1070.

Tian, Y. and Karayiannis, T., 2000. "Low turbulence natural convection in an air filled square cavity: part i: the thermal and fluid flow fields". *International Journal of Heat and Mass Transfer*, Vol. 43, No. 6, pp. 849–866.

Upson, C., Gresho, P. and Lee, R., 1980. "Finite element simulations of thermally induced convection in an enclosed cavity". Technical report, California Univ., Livermore (USA). Lawrence Livermore Lab.

Velusamy, K., Sundararajan, T. and Seetharamu, K., 2001. "Interaction effects between surface radiation and turbulent natural convection in square and rectangular enclosures". *Journal of heat transfer*, Vol. 123, No. 6, pp. 1062–1070.

Versteeg, H.K. and Malalasekera, W., 2007. *An introduction to computational fluid dynamics: the finite volume method*. Pearson Education.

Wang, H., Xin, S. and Le Quéré, P., 2006. "Étude numérique du couplage de la convection naturelle avec le rayonnement de surfaces en cavité carrée remplie d'air". *Comptes Rendus Mécanique*, Vol. 334, No. 1, pp. 48–57.

Yin, S., Wung, T. and Chen, K., 1978. "Natural convection in an air layer enclosed within rectangular cavities". *International Journal of Heat and Mass Transfer*, Vol. 21, No. 3, pp. 307–315.

Yucel, A., Acharya, S. and Williams, M.L., 1989. "Natural convection and radiation in a square enclosure." *Numer heat transfer*, Vol. A15, pp. 261–278.

9. RESPONSIBILITY NOTICE

The authors are the only responsible for the printed material included in this paper.